AN EFFICIENT AIDED DESIGN TECHNIQUE FOR GRID CONNECTED RESIDENTIAL PHOTOVOLTAIC SYSTEMS

M. Djarallah*, B. Azoui

Research Laboratory LEB, Department of Electrical Engineering
Faculty of Sciences Engineering, University of Batna,
Rue Chahid Med Elhadi Boukhlouf, 05000 Batna, Algeria.
* Email: djarmed@yahoo.fr

Abstract: A great progress has been made in the PV material fabrication; however, the evolution in the corresponding design tools is not promoted, especially in the grid connected PV system. So, a more advanced examination is needed for each component, particularly the power conditioning unit (PCU); which is mainly the key element in this system. The success optimal operation of the whole system depends on the decision that any designer has to make for the determination of the power conditioner parameters. This concerns, in particular, systems development and their control strategies, which depend completely on the available design tools and the implantation techniques. In this paper, a set of relatively simple decoupled modelling mathematical formulae, suitable for both, direct current (DC) and alternating current (AC) frames are developed and investigated. These expressions are useful in sizing photovoltaic (PV) arrays and PCU parameters. Also, they allow the determination of the minimum power to be recovered and the corresponding modulation index. Such expressions are validated, then simulated and followed by a discussion of a grid connected PV system case study.

Keywords: grid connected PV systems, stand alone PV systems, MPPT, load operating characteristics, PWM inverter topologies.

1. Introduction

One of the most promising renewable energy technologies is the photovoltaic. There is a growing consensus, stimulating that distributed photovoltaic systems, which provide electricity at the point of use, will be the first to reach widespread commercialisation [1]. The chief one, among these applications, is single-phase grid connected PV power systems for dwellings (*1-5kW*), [2].

In order to identify the significant parameters of such systems, a deeper analytical knowledge is crucial. Herein, analytical tools are prerequisites; Modelling grid connected PV systems, with a set of simple and accurate mathematical formulae, like those developed for stand alone PV systems [3, 4, 5], will progress their development and disseminations.

Fig. 1 shows a typical depiction of such systems, which can be either with or without transformer; this configuration permits: feeding consumers and decreasing the peak demand.

The determination of PCU parameters, referred to the DC or AC frames, is one of the important decision that a grid connected PV system designer has to make; so, the system will operate successfully in the optimal positions. This concerns the hardware parts as well as the control strategies, which depend completely on the available design analytical tools and the implantation techniques. As an example, a poorly designed inverter MPPT algorithms may become lost in their search for the maximum power point [6].

Few authors have studied deeply this subject. In [7, 8], models are developed toward the stability analysis of power electronics based systems, while in [9], AC classical matrix coupled models are used, and a DSP (Digital System Processing) control scheme is implemented. In [10], it is suggested a set of decoupled modelling expressions in the DC side

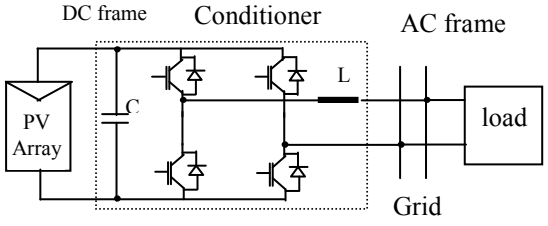

Fig.1: Typical grid connected PV chain

for both inverter output current and power (load) angle; but these expressions are knotty and need precision. In this paper a set of a new decoupled equations, suitable in both frames DC and AC are developed and investigated. Effectiveness of these decoupled extended expressions appears in the system design procedures and performance predictions. Expressions are validated; followed by simulation and discussion of a typical case study.

2. System modeling

To determine the mathematical model of each element of the grid connected PV chain, an equivalent circuit is used (Fig. 2). It is obtained under the following assumptions: the PV array is represented by "one-diode" model, where the shunt resistance is neglected, R and L are the overall parasitic and inverter resistance and filter inductance accounting for any other flux leakage, respectively and system is considered to be in the steady state;

2.1. Classical coupled model

The DC frame model (Fig. 2) contains a current source I_{PH}, one diode and a series resistance R_S which represents the total resistance of the array including that of wiring. The PV array net current I_{PV} is expressed as, [6]:

$$I_{PV} = I_{PH} - I_0\left(\exp(\frac{V_{PV} + I_{PV}R_S}{AkT/q}) - 1\right) \quad (1)$$

where A is the ideality factor, k Boltzmann's gas constant, T the absolute temperature of the array, I_0 the saturation current, q the electron charge and V_{PV} the voltage imposed across the array.

Applying Thevenin theorem between a and b (Fig. 2), the AC equivalent circuit and its vector diagram are given as depicted in Fig. 3. The necessary mathematical expressions for this development are, [6]:

$$I_G = \frac{1}{Z}\sqrt{V_S^2 + V_G^2 - 2V_S V_G \cos\delta} \quad (2)$$

$$\delta = \cos^{-1}\left(\frac{V_G + I_G R}{V_{S1}}\right) \quad (3)$$

$$V_G = V_S(\cos\delta - \frac{R}{X_L}\sin\delta) \quad (4)$$

where Z is the AC side impedance and V_S (=V_{S1}) the inverter fundamental output voltage.

Equation (2) has a great importance in the system design and behavior prediction. This equation gives

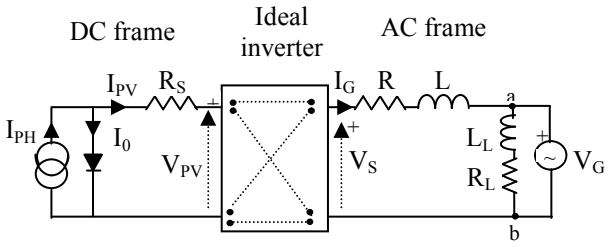

Fig.2: Equivalent circuit of the grid connected PV system

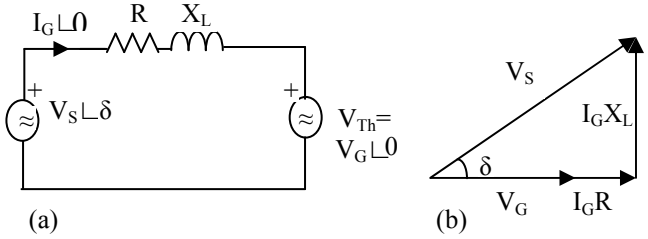

Fig.3: a) AC side equivalent circuit model and b) its vector diagram

the load operating characteristics (LOC) in the AC side; it is an irrational function which has a specific deal (two solutions). It is observed that these equations are non-linear, coupled, and suitable only in the AC side. This is a problematic for any designer dealing with both frames (AC and DC).

2.2. Extended coupled model

The development of this model requests a technique permitting conversion between DC and AC frames; which requires a factor allowing the transition in both directions. Having the previous hypothesises, and using the energy conservation theorem [10, 11], then,

$$P_{PV} = P_{AC} \quad (5)$$

The pulse width modulation (PWM) inverter input and output voltages (current) are related by the amplitude modulation ratio (m). Thus, the expressions for these are [6]:

$$V_S = \frac{m}{\sqrt{2}}.V_{PV} \quad (6)$$

$$I_G = \frac{\sqrt{2}}{m}I_{PV} \quad (7)$$

The generalised transformation technique is obtained using equations (6) and (7), where $\frac{m}{\sqrt{2}}$ is the voltage transformation ratio and $\frac{\sqrt{2}}{m}$ is the current transformation ratio in the transition from AC frame to DC frame.

By applying the transformation technique, the extended equations can be deduced as follows:

The DC current value is mapped using the suitable scaling factor, while the PV voltage is replaced by its corresponding AC voltage, deduced from equation (6). So, the expression of I_{PV} transferred to AC frame is:

$$I_{PVT} = \frac{\sqrt{2}}{m}\left[I_{PH} - I_0 \left\{ \exp\left(\frac{V_{PV} + I_{PV}.R_S}{AkT/q} \right) - 1 \right\} \right] \quad (8)$$

The load operating characteristics, in the DC frame, is always defined in I-V or P-V to cope with that of the PV array characteristics. Consequently, equations (2) and (3) are transferred while equation (4) is adapted. Following are these expressions,

$$I_{GT} = \frac{m}{2Z}\sqrt{m^2 V_{PV}^2 + 2.V_G^2 - 2\sqrt{2}V_{PV}V_G \cos\delta} \quad (9)$$

Equation (9), LOC in DC frame, is used in a single-phase grid connected PV system performance evaluation and prediction.

The remaining expression is:

$$\delta_T = \cos^{-1}\left(\frac{\sqrt{2}(V_G + I_{GT})}{mV_{PV}} \right) \quad (10)$$

The remarks to come across from both equations are: they are coupled, contain mixer of AC and DC parameters. According to these remarks, it is important to find new decoupled equations to solve many problems, such as recovering the minimum injected power, selecting the transformer ratio, etc.

Concerning the minimum injected power problem which is related to the transformer ratio selection, the parameter V_G should be expressed as a function of V_{PV}. The adaptation of equation (4) gives the answer to these requirements. So, the adapted form of equation (4), is:

$$V_G = \frac{m}{\sqrt{2}}V_{PV}\left(\cos\delta - \frac{R}{X_L}\sin\delta \right) \quad (11)$$

This equation has the following important tasks: choosing the maximum value of V_G, determination of the minimum transformer ratio (for PCU with transformer), and recovering the minimum power possible under different climatic conditions.

2.3. Decoupled extended expressions development

Substituting equation (3) into equation (2) and with some rearrangements, equation (12) can be obtained:

$$Z^2.I_G^2 + 2RV_G.I_G - (V_S^2 - V_G^2) = 0 \quad (12)$$

The positive root of this equation, avoiding the collapse area, is:

$$I_G = \frac{1}{Z^2}\sqrt{R^2 + X_L^2\left(1 - \frac{V_G^2}{V_S^2}\right)}.V_S - \frac{R}{Z^2}.V_G \quad (13)$$

Equation (13) is the decoupled LOC in the AC frame, which is a function of R, X_L, V_G and V_S. This equation is suitable for many tasks such as studying the impact of parameters on system behaviour.

The power control angle δ should appear as a parameter in the power expression (I_G). After substituting equation (4) into equation (13), equation (13) becomes as equation (14),

$$I_G = \frac{1}{Z^2}\sqrt{A_1 + A_2}V_S - B \quad (14)$$

where : $A_1 = R^2(1 - \sin^2\delta) + X_L^2(1 - \cos^2\delta)$,

$A_2 = 2.R.X_L.\sin\delta.\cos\delta$, and

$$B = -\frac{R}{Z^2}(\cos\delta - \frac{R}{X_L}\sin\delta).V_S$$

Equations (13) and (14) are suitable to carry out many studies (system sizing, performance evaluation, etc.), especially the analysis of the impact of different parameters on the system behavior. The decoupled equation of the power angle δ in the AC frame can be obtained as:

$$\delta = \cos^{-1}\left[C + \frac{R}{Z^2}\sqrt{R^2 + X_L^2.(1 - \frac{V_G^2}{V_S^2})} \right] \quad (15)$$

Where $C = \frac{X_L^2}{Z^2}.\frac{V_G}{V_S}$

For the purpose of sizing and studying the climatic effects on the performance of the system, it is convenient that equations (13), (14) and (15) to be transferred to the DC frame. To do so, the transformation technique given by equations (6) and (7) is employed. Following are the LOC, δ, and V_G equations in DC frame,

$$I_{GT} = \frac{m^2}{2Z^2}\sqrt{R^2 + X_L^2\left(1 - \frac{2.V_G^2}{m^2 V_{PV}^2}\right)}.V_{PV} - D \qquad (16)$$

where $D = \frac{m.R}{Z^2.\sqrt{2}}V_G$

LOC equation with parameter δ and without V_G, is found by the same procedure from the equation (14),

$$I_{GT} = \frac{m^2}{2Z^2}\sqrt{A_1 + A_2}.V_{PV} - F \qquad (17)$$

where: $F = \frac{m^2}{2Z_L^2}(\cos\delta - \frac{R}{Z_L}\sin\delta)V_{PV}$

The adapted expression for phase angle δ of the inverter output voltage as a function of V_{PV} is found by replacing V_S with its equivalent expression (equation (6) into the equation (15)), so,

$$\delta = \cos^{-1}\left[\frac{X_L^2}{Z^2}\frac{\sqrt{2}.V_G}{mV_{PV}} + \frac{R}{Z^2}\sqrt{R^2 + X_L^2.(1 - 2\frac{V_G^2}{m^2 V_{PV}^2})}\right] \qquad (18)$$

Comparing equations (16) and (18) with those deduced in [10], equations (16) and (18) are: relatively simple and more accurate.

2.4. Decoupled extended model verification

The extended expressions developed previously are to be verified by both calculation and experimentation. Main required conditions, which have to be satisfied during these verifications, are: power conservation theorem, approval of classical models, and approval of the experimentation results of [10].

A *3kW* peak power demand, which can feed any residential type dwelling houses, is selected for the analytical verification .The PV array satisfying this peak demand has *3.112kW*$_P$, configured as: two strings (N_P=*2*), in each string there are *13* modules in series (see appendix) connected to string inverters; which in principal, satisfies the approach followed in this verification.

A. Numerical verification

Two sets of expressions are to be verified; the first set concerns the extended expressions developed for the AC frame, while the second set concerns the transferred ones. The verification of the decoupled extended AC expressions is done by using: P_I = *2800W*, V_G = *220V*, *R=0.3Ω*, *L=9mH*, *m = 0.78* and V_S = 226.693V; with the values of (13) and (14) transferred to the DC side. The results given in table 1 confirm the analytical exactitude of equations (16), (17) and (18). Furthermore, the comparison of the results of the extended expressions with that of the DC referenced values; validates equations (19), (20) and (21). As a final remark, the energy conservation theorem and the approval of classical models are hold for all extended expressions, in both DC and AC frames.

Table 1: Numerical verification

Equations	Results	Comments
(07)	I_G= 12.733A	classical model
(14)	δ = 9.1415°	
(16)	I_G= 12.73A	equal P_I/V_G
(17)	$I_G(\delta)$= 12.7A	equal to eq. (16)
(18)	δ = 9.1414°	equal to eq. (14)
(10)	V_{SDC}=411.0V	DC reference values
(11)	I_{GDC}= 7.025A	
(19)	I_{GT} = 7.0198A	extended model in the DC frame
(21)	δ = 9.1414°	
(20)	$I_{GT}(\delta)$= 7.02A	

B. Validation by comparison

In [10], an experience was carried out to validate the effectiveness of an announced LOC expression. The experimental data used for the verification of I_{GDC} are: P_{DC}=*46.9W*, V_{DC}=*28.6V*, *PI=44.2W*, V_G=*16V*, *R=0.3Ω*, *L=9mH*, and *m = 0.9*. While the ones for δ verification, are: V_S=*30.2V*, *δ=37°*, V_{DC}=*47.5V*, and *m=0.63*.

The results of extended expressions (16, 19, 20 and 21) compared with the experimental analogous data are given in table 2.

Table 2: Validation by comparison

Side	exp.[10] and eqs.	Results	Errors
AC	experience	I_{GAC} = 4.40A	
	eq. (13)	I_{GAC} = 4.4A	0.0023%
	eq.(4) [10]	I_{GAC} = 2.04A	53.64%
DC	exp.	I_{GDC} = 1.7A	
	eq. (16)	I_{GDC} = 1.60A	2.31%
	eq.(4) [10]	I_{GDC} = 2.35	43.24%
	experience	δ = 37°	
	eq. (18)	δ = 35.4	4.32%

exp.: experience and eqs: equations

It can be observed that, the numerical /experimental accuracies of the results obtained in this work are acceptable.

3. Decoupled model investigation

By using the extended expressions, the grid connected PV systems is examined in same procedure like that of the DC direct coupled/stand alone PV systems, especially in characterisation and sizing. The efficiency of each extended expression is clarified by studying the impact of some key parameters, on the performance of the system.

3.1. Simulation and discussion in AC frame

First of all, to show the disadvantages of the classical coupled models, equations (2) and (8) are plotted in the AC frame for $m=0.78$, $\delta=8.5°$, $V_G=220V$. Fig. 4 shows the plots of all LOCs, coupled and decoupled; where the possibility of two operating points A and B (collapse region) for the coupled one. This problem was eliminated by using the decoupled extended equations (13) or (14). It is observed that the similarity of the decoupled LOCs to that of a Stand-Alone PV systems feeding an (*R, L*) impedance with some particularities.

A. Effects of R and L

Since converters, in general, particularly inverters in direct connected PV systems, exhibit negative impedance characteristic, which has detrimental consequences, thereby the effects of these parameters should have this feature. Fig 5 shows the effect of negative impedance, which has a consequence of a diminution injected power. As a result of this simulation, parasitic parameters R and L must be compensated by a selection of the suitable inverter topology or by the maximum power point tracking (MPPT) algorithm.

B. Effect of the angle δ

Fig.6, drawn by using the extended decoupled equation (17), confirms the important task of the inverter output voltage phase angle δ, with respect to the grid voltage, regarding the power transfer.

C. Role of the modulation index m

The amplitude modulation index *m* is the key-parameter for successful and optimal operations of any grid connected PV PWM scheme inverter. In addition to its main task, which is creation of a sinusoidal voltage waveform at a desired frequency, it can be used to follow the MPP as well as to compensate the negative effects of parasitic parameters (*R* and *L*). Thus, prediction and removal of the effects of parasitic parameters by using the decoupled extended equation (13), provides the designer with the full linear range of *m* to control the inverter. All these tasks can not be shown in Fig. 7, but they might be deduced indirectly. Those effects can be observed clearly in the DC frame.

3.2. Simulation and discussion in DC frame

The effect of the modulation index *m*, discussed in the previous section was not completely given, because the AC frame is not suitable for that. The other parameter, which has not been discussed yet, is the selection of the maximum secondary grid voltage V_G.

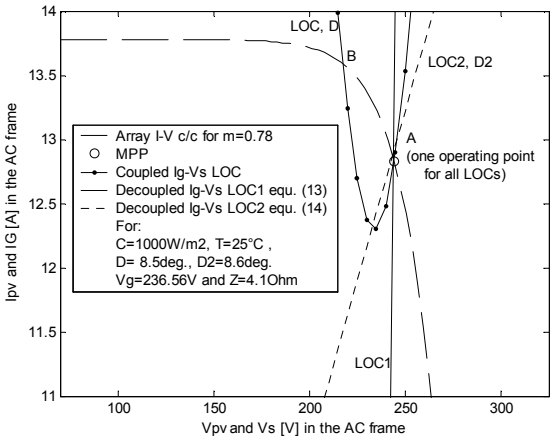

Fig. 4: I-V characteristic (c/c) for PV array at STC associated with LOC(s) in the AC frame.

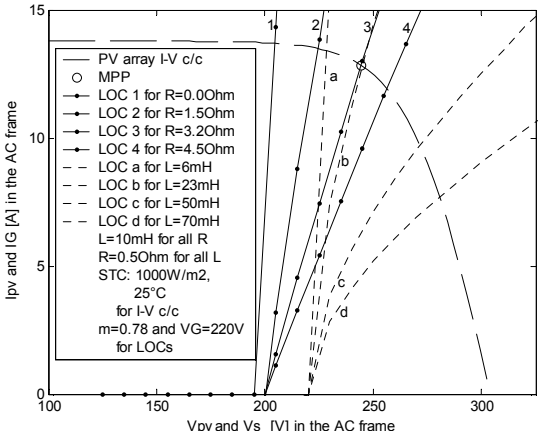

Fig. 5: Consequences of negative impedance on the direct connected PV systems

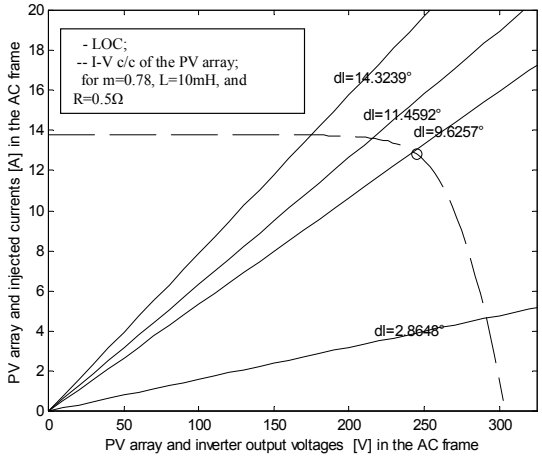

Fig. 6: Modulation index (m) variation effects on the I-V c/c of the PV array

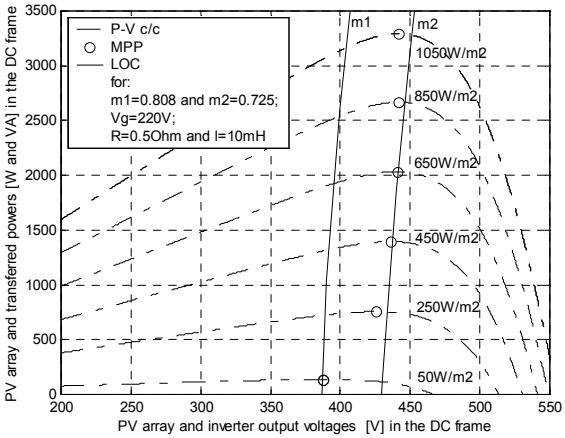

Fig. 8: Modulation index (m) variation effects on the LOC curve in the DC frame

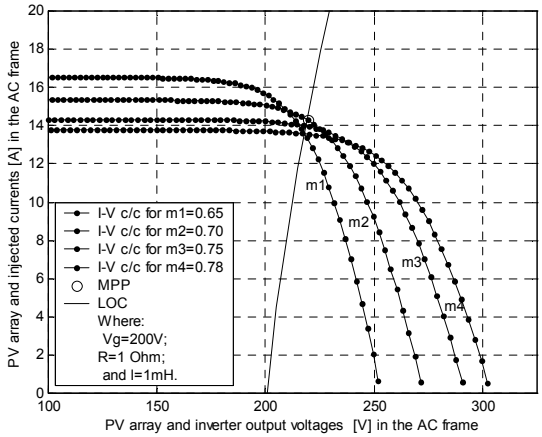

Fig. 7: Modulation index (m) variation effects on the I-V c/c of the PV array

A. Role of the modulation index (m)

To make obvious the tasks of the modulation index exposed in the previous discussions, let draw a family of load curves (equation 16) for a specified range of *m*, associated with that of the PV array as it is shown in Fig. 8; from which the MPP algorithm can detect all the maximum power points for values of *m* located in the interval [*0.725- 0.808*]. If there is an increase, for any circumstances, in parasitic parameters, the negative impedance effect increases as well; then the detection of maximum power point (MPP) corresponds to the smallest value of *m* which is not any more 0.725, but with a value greater than 0.725. Thus, the decrease in the range of *m* should be carried out by the MPPT to compensate the delivered power diminution. Therefore, the detection of MPP for different climatic conditions are done in a narrow interval of *m*, which makes inverter MPPT algorithm inaccurate. For this reason, the minimisation of parasitic parameters in such systems (MPPT included in the inverter control system) is required.

B. Choice of V_G

This discussion concerns the module integrated, the module-oriented or the string self commutated inverters with line frequency transformers. Let take the last topology case, where the PV array structure is formed by one branch of four modules of Solarex MSX-120 at STC (see appendix).

The selection of V_G puts together other intervening parameters (minimum transformer voltage ratio, lowest PV power to be recovered, maximum modulation index and minimum displacement angle δ). Equations (11) and (17) can be used to proceed in these selections as follows: by taking $\delta_{MIN} = 0.1$ radian (normally known), and by the determination of the voltage corresponding to the minimum power to be recovered, (using equation (1)), equations (1) and (17) are solved to determine the maximum modulation index M_{max}; then V_G is computed from equation (11); and finally the transformer ratio N is obtained as $N=\frac{220}{V_G}$.

This procedure has given the following results: the minimum power to be recovered is *18.34W*, the computed corresponding voltage is *68.3V*, the solution of equations (1) and (17) has given the maximum modulation index equal to *0.838*, and finally the calculated V_G is found equal *39.6263*. So, V_G can be taken equals to *40V*, which is confirmed in

Fig.9, as well as in the experimentation results given in [10].

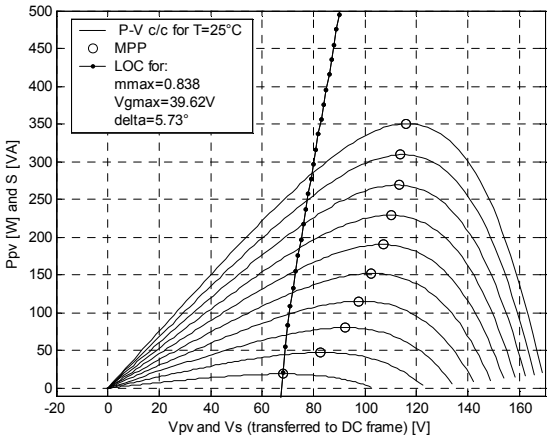

Fig. 9: Numerical results for V_G selection

As a guide line, here are some proposals concerning the grid connected PV applications and the suitable working frame: PV array sizing, prediction of the parasitic parameters, system components dimensioning, and system performance evaluation are preferred to be done in the DC frame; while energy pattern (selling, buying and saving), impact of AC parameters on the system performance, and piecewise static model optimisation in the AC frame.

4. Conclusion

An efficient aided design technique for grid connected residential photovoltaic systems has been developed. A mathematical analysis was carried out on the PCU model, giving straight forward expressions, especially, that of the decoupled load operating characteristics (LOC); where its efficiency was tested experimentally.

In addition to this, other simple expressions are developed for sizing the PV array and most parameters of the PCU with the same procedure, like that of DC direct coupled/stand alone PV systems. Parameter effects are also clearly investigated. It is well worth to mention the proposed procedure to determine the minimum power to be recovered, the corresponding voltage and the consequent modulation index. Finally, a suggested guide line for a grid connected PV system study is given.

References

1. Meinhardt, M.; Cramer, G: *Past, present and future of grid connected photovoltaic- and hybrid-power-systems.* In: Power Engineering Society Summer Meeting, 16-20 July 2000, IEEE, vol.2, 2000, pp.1283-1288.

2. Schramm, G., Kern, E: *Accelerating photovoltaic production through grid connected applications in developing countries*. In: Photovoltaic Specialists Conference, 2000. Conference Record of the Twenty-Eighth IEEE, 15-22 Sept 2000, pp.36-39.

3. Djarallah, M., et al. : *Performance Evaluation of Test Facility and Characteristic Measurement of Photovoltaic Pumping Systems.* In: UPEC00, Belfast, England, 2000.

4. Azoui B., Djarallah M., Hamouda C.,. Chabane M, Hanitsch R., and Duschl G.: *Photovoltaic Pumping System with NdFeB Brushless DC Motor.* In: Electromotion Journal, pp. 19-24, January-March, 2001.

5. Azoui, B., Bekta, A., Djarallah, M., Chabane, M. and Moussi, A.: *Sizing and Optimisation Models for Photovoltaic Pumping System using BLDC Motor.* In: AMSE, 2003, pp.55-68.

6. Hudson, R. et al.: *Design Considerations for Three-Phase Grid Connected Photovoltaic Inverters*. In: Photovoltaic Specialist Conference, 2002, Conference Record of the Twenty- Ninth IEEE, pp.1396-1401.

7. Steven, F. G.: *Modeling and stability analysis of power electronics based systems*. In: PhD thesis, Purdue University, May 2003.

8. Li Wang, Ying-Hao Lin.: *Random fluctuations on dynamic stability of a grid-connected photovoltaic array.* In: Power Engineering Society Winter Meeting, 2001. IEEE vol. 3, 28 January- 1 Febrery 2001, pp.985-989.

9. Sivakumar, S, et al.: *Modeling, analysis and control of bidirectional power flow in grid connected inverter systems.* In: Proceedings of the Power Conversion Conference, PCC'02 Osaka, 04-05 May 2006, vol.3, pp.1015-1019.

10. Scapino, F, Spertino, F.: *Load curves at DC inverter side: a useful tool to predict behavior and aid the design of grid-connected photovoltaic systems*. In: Proceedings ISIE'02, IEEE, 26-29 May 2002, pp.981-986.

11. J. C. Alfonso-Gil, et al,: *New Optimization In Photovoltaic Installations With Energy Balance with the Three-Phase Utility*. In:, 2005. Proceedings of the IEEE International Symposium on Industrial Electronics, Vol. 3, Issue, 20-23 June 2005, pp. 981 – 987.

Appendix

The PV module, Solarex MSX-120, characteristics used for calculations and simulation at Standard Test Conditions (STC: 1000W/m^2, *AM 1.5*, and *25°C*) are:
Open circuit voltage $V_{oc} = 42.6V$;
Rated power $P_{mpp} = 120\ W_p$;
Rated voltage $Vmpp = 34.2V$;
Rated current $Impp = 3.5A$;
Open circuit voltage $Voc = 42.6V$;
Short circuit current $I_{sc} = 3.8A$;
Series resistance $R_S = 0.71\Omega$;
Saturation current at 20 °C $I_0 = N_p$x17 nA;
Diode quality factor $A = 1.2$
Number of cells/ module = 72
I_{sc} temperature coefficient $\alpha = 6.0\ mA/°C$;
V_{oc} temperature coefficient $\beta = -146\ mV/°C$